Article

Anti-Frothing Effect of Poultry Feathers in Bio-Based, Polycondensation-Type Thermoset Composites

Markus Brenner [1], Crisan Popescu [2] and Oliver Weichold [1,*]

[1]   Institute of Building Materials Research, Schinkelstraße 3, 52072 Aachen, Germany;
      brenner@ibac.rwth-aachen.de
[2]   Kao European Research Laboratories, KAO Germany GmbH, Pfungstädter Str. 98–100, D-64297 Darmstadt,
      Germany; crisan717@yahoo.co.uk
[*]   Correspondence: weichold@ibac.rwth-aachen.de

check for
updates

Featured Application: Potential green alternative to petrochemical thermoset resins in the fields of adhesives and fibre-reinforced composites.

Abstract: The formation of polycondensation-type thermoset resins from natural reactants such as citric and glutaric acid, as well as 1,3-propanediol and glycerol, was studied. Monitoring the mass loss by thermogravimetric analysis (TGA) allowed the rate constants of the esterification to be calculated, which were in the order of $7 \cdot 10^{-5}$ s^{-1} for glutaric acid and approximately twice as high for citric acid. However, the combination citric acid/glycerol was previously reported to froth up at high conversions, giving rise to foams, which makes the preparation of compact engineering composites challenging. In light of this, we observed that shredded poultry feathers not only increased the conversion and the reaction rate of the combination citric acid/glycerol, but increasing the amount of feathers continuously decreased the number of visible bubbles. The addition of 20 wt% of feathers completely prevented the previously reported frothing and gave rise to compact materials that were macroscopically free of defects. Besides this, the addition of feathers also improved the fire-retardant properties. The tensile properties of the first specimens are still rather low (σ = 11.6 N/mm^2, E = 750 N/mm^2), but the addition of poultry feathers opens a new path for green thermoset resins.

Keywords: thermoset; polyester; bio-based; poultry feathers; composite

1. Introduction

Thermoset resins are an important class of materials for adhesives [1] and load-bearing matrices in fibre-reinforced composites [2]. Typical examples are phenolic and epoxy resins, polyurethanes, unsaturated polyesters, or silicone rubbers [3]. However, the main source for these polymers is petrochemical feedstock and only very few attempts at a partial substitution by renewable materials, such as epoxidised castor and soybean oils [4], or bio-based polyols [5], have received wider attention. On the other hand, the growing environmental awareness and recent governmental regulations have increased the pressure on industry and academia to focus more on renewable and sustainable materials, closed material cycles, and materials with low or, ideally, zero carbon footprints. One reason for the difficulties in replacing petrochemical resources with natural ones, when it comes to thermoset resins, is the required high reactivity. Nature usually circumvents highly reactive functional groups, such as isocyanate and epoxy, by using highly specialised enzymes as catalysts in condensation reactions. As a result, bio-based feedstock requires in vitro reaction conditions not directly compatible with the requirements for thermoset resins. Thus, it seems that natural building blocks would not be suitable for making thermoset resins. However, the vast amount of natural or bio-based polyacids and polyols

merits a closer look: by esterification, which is generally a rather slow, only slightly exothermic reaction type generating a lot of water as by-product, bio-based seminal thermoset materials were successfully generated, as presented in this paper.

Quite a common example of such an esterification is poly(butylene succinate), which can be synthesised from succinic acid and 1,4-butanediol via polycondensation and goes back to the work of Carothers [6]. Ever since, the polycondensation reaction has been refined and optimised, in particular to include new monomers and more active catalysts [7]. A recent example is the synthesis of a thermoset resin from lactic acid and glycerol, which was used to impregnate regenerated viscose fibre and compression-moulded to form a thermoset composite [8]. Naturally available di- and multifunctional carboxylic acids have been used to cross-link epoxidized sucrose soyate in order to produce a thermoset polyester that rapidly degrades in dilute sodium hydroxide [9]. A promising material is the combination citric acid and glycerol. Polymerised in solution at molar ratios from 0.75 to 1.5, the material obtained was initially an insoluble amorphous solid, that dissolves in water within 8 to 10 days and can be bio-degraded by *Aspergillius niger* and *E. coli* [10]. A material produced from citric acid and glycerol without a catalyst was used as a degradable thermoset polymer for drug delivery applications [11]. However, when prepared in bulk, the material turns out liquid, gel-like, or as an inhomogeneous foam due to the evaporation of substantial amounts of water as steam [12]. To the best of our knowledge, a catalysed method to produce compact solids from this mixture is not known.

Another aspect of substituting petrochemical feedstock with renewable resources is the exploitation of natural waste materials. Among these, poultry feathers are an interesting class, since they have one of the highest fracture toughnesses in nature [13] and make up approximately 10% of the weight of poultry [14]. This is a problem in poultry farms, because huge amounts of feather waste are generated, which are taken to landfills for disposal. The estimated global annual amount of feathers produced in poultry farms is in the order of 4 million tons [15]. Consequently, several research groups have studied the re-use of poultry feathers, e.g., in composite materials. Aranberri reported lightweight, biodegradable composites of polylactic acid or poly(butyrate adipate terephthalate) with up to 60 wt% poultry feathers, which were proposed as an insulation material [16]. Barone investigated the process parameters for compounding polyethylene and shredded feathers and found that feathers only act as reinforcements in polyethylene of low crystallinity [17,18].

Here, we present the first results of our work to bring these two topics together. It is our firm belief that polycondensation resins based on the above or similar natural or bio-based reactants can, at least in part, be an environmentally friendly alternative to petrochemical thermoset resins, provided that methods to circumvent the difficulties with evaporating condensation products are found. Citric and glutaric acid, as well as 1,3-propanediol and glycerol, are used as model ester resins, which liberate water during the reaction. Shredded poultry feathers are incorporated, because their dendritic structure and moisture sorption properties are expected to help in solving the problem caused by the generation of large amounts of water as by-product. Additionally, we expect the feathers to also improve the thermal and mechanical properties of the composites.

2. Materials and Methods

Citric acid, 1,3-propandiol, glutaric acid, and tetra-n-butyl ortotinanate were used as received. Glycerol was dried at 170 °C for three hours. Figure 1 shows the structures and abbreviations of the materials used. Goose feathers were provided washed and dried by a local manufacturer and shredded using a Retsch SM300 cutting mill with a 0.5 mm sieve. Prior to use, the feather shreds were dried at 120 °C for one hour.
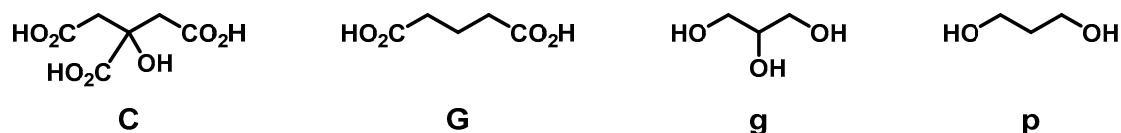
Figure 1. Structures and abbreviations of the compounds used to prepare the polyesters (C = citric acid; G = glutaric acid; g = glycerol; p = 1,3-propanediol). For example, the reaction of citric acid and 1,3-propanediol in a 1:1 molar ratio as well as the resulting product are labelled Cp1-1.

2.1. Polyester Preparation

The preparation of all mixtures followed a general procedure, which is illustrated using Cg1-1 (equimolar mixture of citric acid and glycerol) as an example: 7.04 mmol (1.53 g) citric acid was mixed with approximately half of the equimolar amount of glycerol (equimolar amount: 7.04 mmol, 0.65 g) and slowly heated to 110 °C while stirring. Meanwhile, 106 μmol (35.9 mg) Ti(O*n*Bu)$_4$—equivalent to 0.5 mol% per OH group—was added to the remaining glycerol. When the mixture of citric acid and glycerol was clear and homogeneous, the glycerol containing the catalyst was added and the combined mixture was stirred for 1 min at 110 °C to ensure complete mixing. For Cp2-3 and Gg3-2, the molar amounts of acid and alcohol were adjusted accordingly. Glutaric acid could be melted without addition of the alcohol.

At this point, the mixtures could be used for differential scanning calorimetry (DSC) and thermogravimetric analysis (TGA) analyses, cast directly into dog-bone shaped silicone moulds, or mixed with feather shreds prior to casting.

2.2. Feather Composite Preparation

The desired amount of feather shreds was weighed into a flask and the freshly prepared hot polyester mixture described above was added under continuous stirring. Mixing was continued for five minutes to ensure a homogeneous distribution of the shreds. During this time, the temperature needed to be kept above 60 °C to prevent solidification of the polyester. The mixture was then poured into 60 °C warm, dog-bone shaped silicone moulds. For curing, the moulds were covered with anti-adhesive paper, followed by a 2 mm thick, water-permeable, non-woven fabric, and an 18 mm screen-printing plate. The complete set-up was loaded with 750 g per sample and placed in a vacuum oven at 120 °C and 20 mbar for 20 h (Figure 2). After cooling in air, the samples could be removed from the mould. Gg samples were then heated for another 48 h at 120 °C.
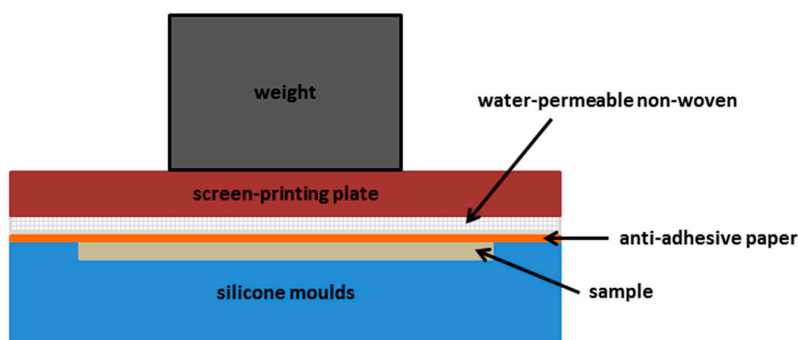

Figure 2. Experimental setup for composite preparation.

2.3. ATR-FTIR Spectroscopy

Infrared IR spectra were recorded using a Perkin Elmer Spectrum Two UATR FTIR spectrometer equipped with a diamond ATR (attenuated total reflection) window. All spectra were recorded in the spectral range of 4000–400 cm^{-1} with 12 scans at a spectral resolution of 4 cm^{-1}. Before each measurement, the diamond ATR crystal was cleaned with isopropanol.

2.4. DSC

The differential scanning calorimetry (DSC) measurements were performed on a Netsch DSC 204 F1 Phoenix. Approximately 40 mg of freshly prepared sample was placed in an aluminium sample pan and the heat flow was recorded between 5 and 170 °C. Each system was analysed at heating rates of 5, 10, 20, and 40 °C/minute. The measurements were carried out under nitrogen atmosphere with a flow rate 20 mL/minute.

2.5. Thermogravimetric Analysis (TGA and TGA-FTIR)

The mass loss during polycondensation was recorded using a Perkin Elmer TGA-4000. Approximately 40 mg of freshly prepared sample was placed in an aluminium oxide sample pan used for TGA. Each system was kept at 10 °C for 5 min, then heated to 120 °C at 10 °C/min, and finally kept at 120 °C for 14 h. The measurements were carried out under nitrogen atmosphere with a flow rate of 20 mL/min as sample purge. Coupled TGA/FTIR measurements were performed by using a Perkin Elmer TL8000 gas transfer line setup with Perkin Elmer Spectrum 2 FTIR spectrometer. A gas transfer line temperature and gas chamber temperature of 270 °C was used. The gas flow used for FTIR measurements was 37 mL/minute, which was two-thirds of the accumulated gas flow in the TGA sample chamber.

To evaluate the thermal stability of the composites, approximately 20 mg of the sample was put into the crucible, conditioned at 30 °C for 5 min, and then heated to 850 °C with a rate of 10 °C/min in a continuous stream of nitrogen or oxygen at a flow rate of 20 mL/min.

2.6. Mechanical Testing

Tensile tests were carried out on an Instron 5566 by using dog-bone shaped samples according to DIN EN ISO 527-2 type 1A and the sample holder shown in Figure 3. The tests were run strain-controlled using a strain rate of 1 mm/min. Recording started when the applied load reached 5 N.
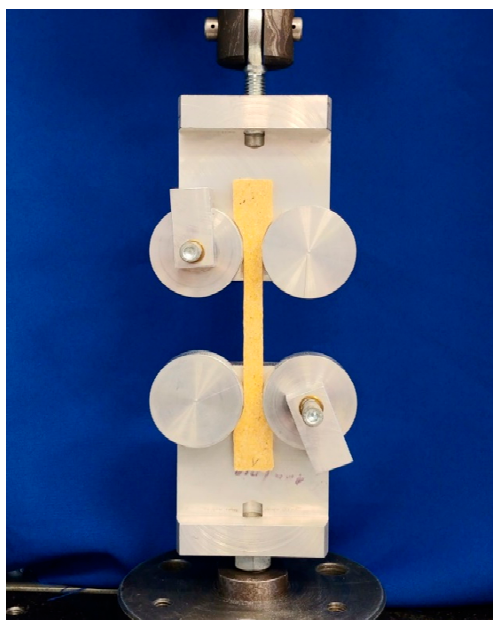

Figure 3. Set-up for mechanical testing.

3. Results and Discussion

The polycondensation was affected by titanium-catalysed esterification of the model compounds in bulk (Figure 4). The formation of ester bonds was confirmed by ATR-FTIR spectroscopy (Figure 5). For glutaric acid, the symmetric stretching vibration of the carbonyl group was observed at 1687 cm^{-1},

and shifted to higher wave numbers upon esterification (Figure 5 left). Citric acid exhibited two bands, at 1695 cm^{-1} and 1743 cm^{-1} (Figure 5 right), which merged into a single band at intermediate wave numbers of 1727 cm^{-1} for Cp1-1 and 1722 cm^{-1} for Cg1-1. This appears to be a common feature of citric acid ester, as triethyl citrate and tributyl citrate also showed only a single band at approximately 1740 cm^{-1} [19]. The carboxylic acid band was hardly visible in the products Gg1-1, Gp1-1, and Cp1-1, indicating high conversions [20]. In contrast, the ester band of Cg1-1 was comparatively broad and could hide some of the original acid bands.
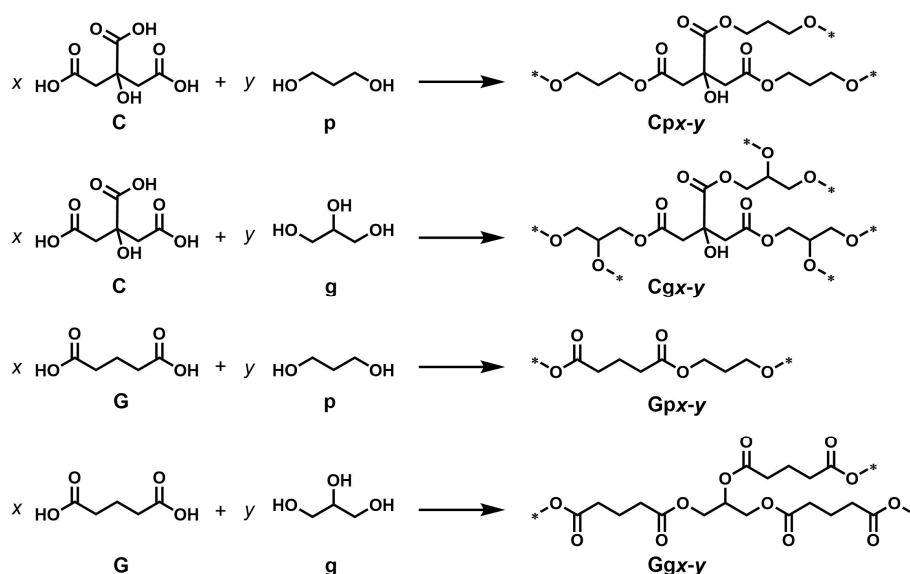

Figure 4. Schematic representation of the four reactions under investigation. x, y represent the stoichiometric coefficients in accordance with Equation (2). A star at the end of a bond indicates continuation of the polymer.
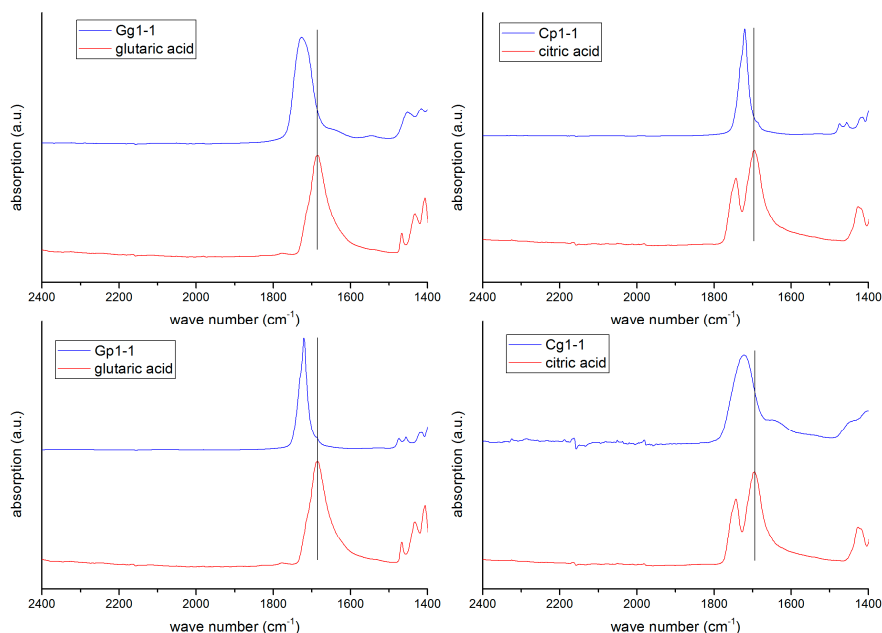

Figure 5. Comparison of the ATR-FTIR spectra of glutaric acid (left) and citric acid (right) with the four principal polycondensation products.

In order to assess the thermodynamic parameters for the polycondensation reactions in Figure 4, the reactions were monitored by DSC at four different heating rates (Figures S1–S4 in the Supplementary

Material). As expected for non-isothermal kinetics [21], the signal observed in the reactions Cp, Gp, and Gg shifted to higher temperatures when increasing the heating rate from 5 to 40 °C/min. However, the lack of effects in the DSC trace of the Cg mixture and the lack of any effects upon cooling and re-heating suggest that these might not relate to the polycondensation reaction shown to occur in all these systems. This is also supported by a comparative evaluation of DSC and TGA traces, exemplified for the Cp1-1 reaction in Figure 6.
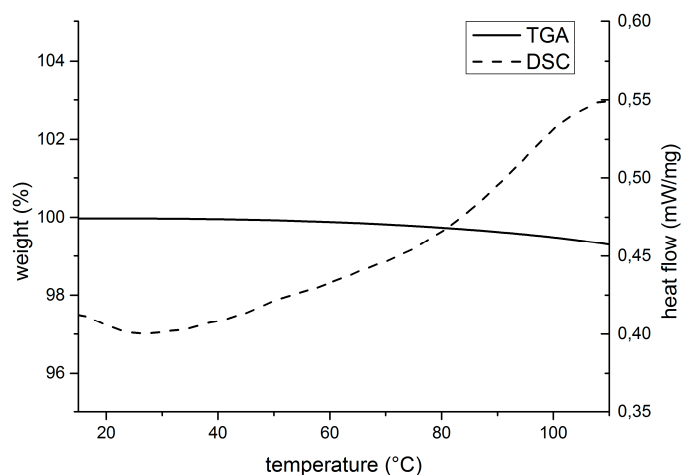

Figure 6. Comparison of DSC (dashed line) and TGA (solid line) traces of the Cp1-1 reaction up to the onset of the isothermal phase.

Clearly, the onset of the signal in the DSC trace at around 100 °C corresponded with the beginning of a mass loss observed by TGA that totalled approximately 2% and thus, could not be caused by the polycondensation reaction. This was further corroborated by monitoring the evaporating reaction products using a combined TGA-FTIR method (Figure 7). During the very early stages of the reaction, the IR spectrum showed, besides the prominent resonances of water vapour, others at 2946 cm^{-1} and 1046 cm^{-1}, indicating aliphatic C-H bonds (Figure 7a). These resonances disappeared not long after their first detection (Figure 7b). The most likely source of aliphatics is the catalyst Ti(OnBu)$_4$, which reacted in the early stages of the polycondensation with either the alcohol or the carboxylic acid to displace n-butanol [22]. In addition, the weight loss of approximately 2% was in accordance with the amount of catalyst used.
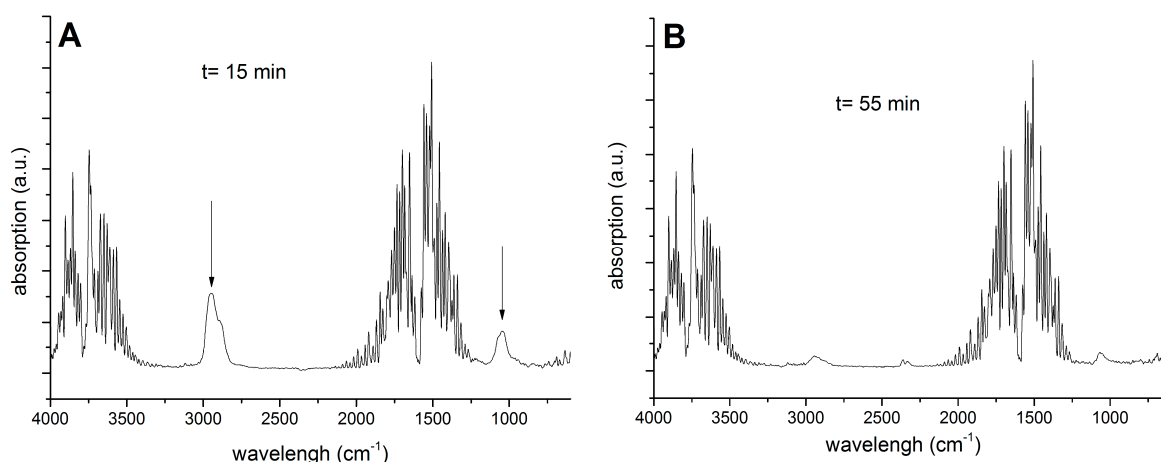

Figure 7. Gas-phase IR used to monitor the isothermal Cp reaction at 120 °C after 15 (**A**) and 55 (**B**) min. Arrows in A indicate the occurrence of *n*-butanol.

In consequence of the above findings, the kinetic parameters of the polycondensation reactions were evaluated using isothermal experiments monitored by TGA (Figure 8). The mass loss in the Gp1-1 reaction was considerably larger than in the other reactions. This is due to the joint evaporation of water and 1,3-propanediol—vapour pressure approximately 10 hPa at 100 °C as opposed to, e.g., 0.02 hPa for glycerol [23], which was confirmed by the combined TGA-FTIR method. On the other hand, 1,3-propanediol was not found to evaporate in the Cp reaction. The reason for this is not entirely clear, but could be caused by stronger hydrogen bonding in the Cp system. A potential alternative explanation is provided further below.
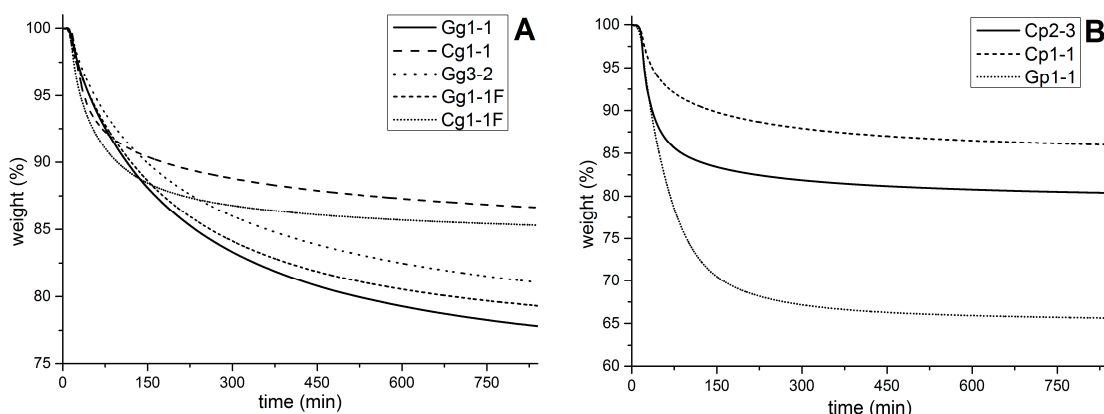

Figure 8. Mass loss of the polycondensation reactions of Figure 4 with glycerol (**A**) or 1,3-propanediol (**B**), as monitored by TGA.

All systems reached the equilibrium within approximately 14 h at 120 °C (Figure 8). The mass loss at equilibrium can be converted to the number of water molecules n liberated during the reaction by solving:

$$\text{TGA mass loss (\%)} = \frac{n_{\text{water molecules eliminated}} \cdot 18 \frac{\text{g}}{\text{mol}}}{M_{\text{acid}} + M_{\text{polyol}}} \times 100\%, \tag{1}$$

where M_{acid} and M_{polyol} are the molecular weights of the corresponding acid and alcohol. Based on the functionality of the reactants (it should be noted that in all calculations, the 2-hydroxy group of citric acid was considered to be unreactive) and the stoichiometry, the mixtures could liberate a maximum of either two or three water molecules. As can be seen from Table 1, some of the mixtures came close to the theoretical number (Table 1, entries 1, 2, 8), indicating that these reactions ran almost to completion. This is not too surprising for the system Cp1-1, for example, which, due to the excess of acid groups, should only form branched polymers with an average degree of polymerisation of 5. However, the systems Cp2-3 (Table 1, entry 2) and Gg3-2 (Table 1, entry 8) went to almost complete conversion, whereas Cg1-1 (Table 1, entry 3) appeared to stop at approximately 57%. This is in accordance with the results from IR spectroscopy (Figure 5). All three systems had a 1:1 ratio of functional groups and could give rise to highly cross-linked materials. Calculating the functionality factor f_{ar} according to:

$$f_{\text{ar}} = \frac{x \cdot p + y \cdot q}{x + y}, \tag{2}$$

where x, y are the stoichiometric coefficients and p, q the number of functional groups of acid and alcohol [24], afforded $f_{\text{ar}} = 2.4$ for Cp2-3 and Gg3-2, while for Cg1-1 $f_{\text{ar}} = 3$. According to the theory of non-linear step-growth reactions, gelation—i.e., the formation of a 3D network—occurs when the degree of polymerisation becomes infinite, and the corresponding limiting conversion p_G is given by $p_G = 2 \cdot f_{\text{ar}}^2$ [24]. This could be calculated as 83% for Cp2-3, Gg3-2 and 67% for Cg1-1. The latter is greater than the conversion determined by TGA (57%), indicating that the 3D network did not fully develop under the applied curing conditions. It can be easily observed during the reaction that the viscosity in

the Cg1-1 system increased rather quickly. The reason for the low conversion in this reaction could, therefore, be the formation of a more rigid framework already at low conversions due to the dense packing of three functional groups in both reactants. This immobilises the chain ends and prevents them from meeting. Conversely, if one of the reactants is less crowded, such as 1,3-propanediol or glutaric acid in the Cp and Gg systems, the reaction reaches high conversions. It is not clear why for the Gg1-1 reaction the mass loss at equilibrium indicates the liberation of 2.5 water molecules, while theory calls for only 2. The joint evaporation of water and one of the reactants can be ruled out in the same way as wet reactants.

Table 1. Results of the kinetic evaluation using pseudo first order kinetics.

Entry	System [a]	Mass Loss at Equilibrium/%	n [b]	n_{theo} [c]	k/s^{-1}
1	Cp1-1	12	1.8	2	1.2×10^{-4}
2	Cp2-3	17	2.9	3	2.4×10^{-4}
3	Cg1-1	11	1.7	3	1.2×10^{-4}
4	Cg1-1F [d]	17 [e]	2.1	3	1.6×10^{-4}
5	Gp1-1	– [f]	– [f]	2	– [f]
6	Gg1-1	20	2.5	2	7.5×10^{-5}
7	Gg1-1F [d]	25 [e]	3.1	2	– [g]
8	Gg3-2	17	2.7	3	7.2×10^{-5}

[a] Abbreviations according to Figure 1; [b] number of water molecules calculated according to Equation (1); [c] theoretical amount of water molecules based on the stoichiometry; [d] mixture containing 20 wt% of feather shreds; [e] value calculated with regard to the feather content; [f] value not calculated due to the joint evaporation of water and diol; [g] value not calculated due to decomposition.

The mass loss over time in the isothermal regime followed an exponential decay, indicating first order kinetics. Although esterification is a classic example of a second order reaction, the use of only 0.5 mol% of the catalyst per OH group of the polyol resulted in a rather low concentration of active centres. This caused the mechanism to follow a pseudo first-order law, under the assumption that autocatalysed esterification was rather slow. Modelling the elimination of water according to:

$$\frac{dm}{dt} = -k \cdot m_0 \cdot t, \tag{3}$$

the TGA curves in Figure 6 can be fitted by rearranging Equation (1) to:

$$\text{TGA mass loss } (\%) = e^{-k \cdot t}. \tag{4}$$

Evidently, the reactions with citric acid were approximately twice as fast as those with glutaric acid. A potential reason for this could be the intramolecular formation of cyclic anhydrides of citric acid under the action of titanium catalysts such as Ti(OnBu)$_4$ [25]. The difference in reaction rates could also facilitate the evaporation of 1,3-propanediol from the Gp1-1 and impede evaporation from the Cp1-1 reaction mixture.

The addition of feathers caused an increase in both the reaction rate and conversion for the Cg1-1 system (Cg1-1F, Table 1, entry 4). The reason for this could be manifold, the simplest one being the vast number of different functional groups provided by the feather keratin, which could open up a number of alternative reaction pathways. Alternatively, the dendritic network of barbules might help in letting the water vapour escape the viscous mixtures and/or the feather keratin might absorb the moisture from the hot mixture. While the latter two would shift the equilibrium to the side of the products (increase of n), the former would increase the reaction rate. Thus, a combination of these alternatives is most likely.

Similar beneficial effects could not be observed when adding feather shreds to the Gg1-1 mixture (Gg1-1F, Table 1, entry 7). While the parent Gg1-1 mixture (Table 1, entry 6) was pale yellow and

transparent, the addition of feathers caused the mixtures to turn reddish-brown (Figure S5 in the Supplementary Material). This apparent decomposition was also manifested in the rather large mass loss at equilibrium of 25%, which can be calculated as a total of three water molecules being liberated per molecule glutaric acid, while in theory it should only be two. Although citric acid is approximately one order of magnitude more acidic than glutaric acid, a similar decomposition was not observed in the Cg1-1F system and this could be due to the esterification occurring faster.

From the above mixtures, those based on citric acid appear more suitable for the preparation of engineering materials, particularly the Cg1-1 combination. However, the combination of citric acid and glycerol is known to froth massively, which prevents the formation of compact workpieces [12]. A plausible reason is that due to the rapid increase in viscosity already at low conversions, most of the water formed in the condensation reaction is trapped inside the viscous mixture in the form of bubbles. Based on the positive effects on the kinetics observed in the Cg1-1F system, the incorporation of shredded feathers was thought to enable the preparation of compact test specimens from citric acid and glycerol for the first time. Indeed, increasing the amount of feathers incorporated into Cg1-1 mixtures clearly reduced frothing and the number of visible bubbles, such that with 20 wt% of feathers, compact and macroscopically defect-free samples could be obtained (Figure 9). The incorporation of higher amounts of feathers appears possible and could potentially give rise to materials with improved properties, but requires more sophisticated mixing techniques.

Figure 9. The Cg1-1 series containing an increasing amount of shredded feathers cured in dog-bone shaped moulds. From left to right: 0 (Cg1-1), 5, 10, 15, and 20 wt-% (Cg1-1F).
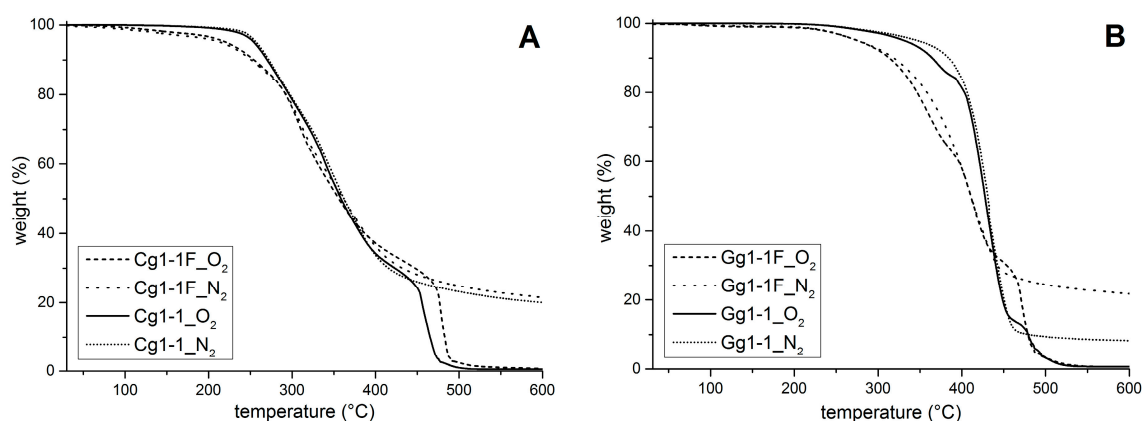
The Cg1-1F samples were obtained as solid and hard, but also rather brittle objects, which made testing in the set-up shown in Figure 3 somewhat difficult. It should be noted that all Cg1-1F samples failed close to the receiving rollers (cf. Figure S6 in the Supplementary Material), most likely because they did not fit precisely to the curvature of the specimen. This indicates that the properties shown in Table 2 and Figures S7–S10 do not represent the best performance of the tested materials. For comparison, the Gg1-1F and the Gg1-1 mixtures were also cured in dog-bone shaped moulds and tested. Due to the lower degree of cross-linking, both specimens were rubbery.

Table 2. Tensile properties of three samples from Table 1.

Sample	Number of Samples	Tensile Strength (N/mm^2)	Stiffness (N/mm^2)
Cg1-1F [a]	3	11.6 ± 2.06	730 ± 55.8
Gg1-1F [a]	3	1.20 ± 0.41	28.13 ± 10.9
Gg1-1	2	0.44 ± 0.13	2.58 ± 0.27

[a] Samples containing 20 wt% shredded feathers.

The thermal stability of the composites was investigated by TGA measurements under both nitrogen and oxygen atmosphere (Figure 10). The former represents rather a pyrolysis, the latter a combustion. Generally, the decomposition temperatures of the samples based on glutaric acid were approximately 100 °C higher than those based on citric acid. The reason for this might be the rather low decomposition temperature of citric acid of 175 °C, where it is transformed to aconitic acid by the elimination of water [26]. Under the assumption made above that the 2-hydroxy group does not participate in the polycondensation, a similar start to the decomposition appears likely for the citrate esters. Under oxygen, all samples were completely burnt at approximately 550 °C, while under nitrogen, a substantial residue remained. From this, the limiting oxygen index (LOI) can be calculated according to LOI = 17.5 + 0.4 · *cr*, where *cr* is the char residue at 850 °C in percentage (Table 3) [27].

Figure 10. Thermogravimetric analysis of the products Cg1-1 (**A**) and Gg1-1 (**B**) with and without 20 wt-% feathers under nitrogen and oxygen atmosphere.

Table 3. TGA data and the calculated limiting oxygen index (LOI).

Sample	Char Residue at 850 °C	LOI/%
Cg1-1	12.304	22.4
Cg1-1F [a]	14.871	23.4
Gg1-1	6.761	20.2
Gg1-1F [a]	16.858	24.2

[a] Samples containing 20 wt% shredded feathers.

The addition of shredded feathers increased the LOI in all cases, and based on the observed values, Cg1-1F and Gg1-1F were considered to be hard to ignite and self-extinguishable in air. It should be noted that the decomposition of Gg1-1F under both nitrogen and oxygen started at considerably lower values than that of Gg1-1 (cf. Figures S11 and S12 in the Supplementary Material). As stated above, the Gg1-1 mixtures containing feathers turned reddish-brown during curing (Figure S5 in the Supplementary Material), which indicates undesired side-reactions that seem to affect the onset of decomposition, but not the fire-retarding properties.

4. Conclusions

In the quest for green alternatives to petrochemical feedstock, this article describes a significant step forward in the technologically important field of thermoset resins. The addition of shredded poultry feathers allowed, for the first time, the exploitation of natural or bio-based feedstock in the form of polyacids and polyols for the production of engineering composites from polycondensation-type thermoset resins. In the first results presented here, the feathers appeared to prevent the previously reported frothing of highly cross-linked combinations, such as citric acid/glycerol, and improved the thermal properties. However, the tensile properties of materials based on this mixture are so far rather low, and IR along with kinetic data indicate the conversion at equilibrium being below the conversion necessary to form a cross-linked 3D network. Improvements in processing and curing will allow the feathers to be activated as reinforcements, which will improve the mechanical properties.

Supplementary Materials: The following are available online at http://www.mdpi.com/2076-3417/10/6/2150/s1, From Figure S1 to Figure S12. DSC traces of the reactions Cg1-1, Cp1-1, Gg1-1, and Gp1-1, optical appearance of specimen Gg1-1 and Cg1-1 after fracture, stress-strain curves from which the results in Table 2 were calculated, and DTG curves for the mixtures Gg1-1 and Cg1-1.

Author Contributions: Conceptualization, O.W. and M.B.; formal analysis, C.P. and O.W.; investigation, M.B.; writing—original draft preparation, all authors; writing—review and editing, all authors. All authors have read and agreed to the published version of the manuscript.

Conflicts of Interest: The authors declare no conflict of interest.

References

1. Engels, T. Chapter 10—Thermoset Adhesives. In *Thermosets*, 2nd ed.; Guo, Q., Ed.; Elsevier: Amsterdam, The Netherlands, 2018; pp. 341–368.
2. De, S.K.; White, J.R. *Short Fibre-Polymer Composites*; Woodhead Publishing: Cambridge, UK, 1996.
3. Hanna, D.; Goodman, S.H. *Handbook of Thermoset Plastics*; William Andrew: Amsterdam, The Netherlands, 2013.
4. Tan, S.G.; Chow, W.S. Biobased Epoxidized Vegetable Oils and Its Greener Epoxy Blends: A Review. *Polym.-Plast. Technol. Eng.* **2010**, *49*, 1581–1590. [CrossRef]
5. Li, Y.; Luo, X.; Hu, S. Introduction to Bio-Based Polyols and Polyurethanes. In *Bio-Based Polyols and Polyurethanes*; Springer: Berlin/Heidelberg, Germany; Cham, Switzerland, 2015; pp. 1–13.
6. Carothers, W.H. Polymerization. *Chem. Rev.* **1931**, *8*, 353–426. [CrossRef]
7. Xu, J.; Guo, B.H. Poly (Butylene Succinate) and Its Copolymers: Research, Development and Industrialization. *Biotechnol. J.* **2010**, *5*, 1149–1163. [CrossRef] [PubMed]
8. Esmaeili, N.; Bakare, F.O.; Skrifvars, M.; Afshar, S.J.; Åkesson, D. Mechanical Properties for Bio-Based Thermoset Composites Made from Lactic Acid, Glycerol and Viscose Fibers. *Cellulose* **2015**, *22*, 603–613. [CrossRef]
9. Ma, S.; Webster, D.C. Naturally Occurring Acids as Cross-Linkers to Yield Voc-Free, High-Performance, Fully Bio-Based, Degradable Thermosets. *Macromolecules* **2015**, *48*, 7127–7137. [CrossRef]
10. Pramanick, D.; Ray, T.T. Synthesis and Biodegradation of Copolyesters from Citric Acid and Glycerol. *Polym. Bull.* **1988**, *19*, 365–370. [CrossRef]
11. Halpern, J.M.; Urbanski, R.; Weinstock, A.K.; Iwig, D.F.; Mathers, R.T.; Von Recum, H.A. A Biodegradable Thermoset Polymer Made by Esterification of Citric Acid and Glycerol. *J. Biomed. Mater. Res. Part A* **2014**, *102*, 1467–1477. [CrossRef]
12. Tisserat, B.; O'kuru, R.H.; Hwang, H.; Mohamed, A.A.; Holser, R. Glycerol Citrate Polyesters Produced through Heating without Catalysis. *J. Appl. Polym. Sci.* **2012**, *125*, 3429–3437. [CrossRef]
13. Wegst, U.G.K.; Ashby, M.F. The Mechanical Efficiency of Natural Materials. *Philos. Mag.* **2004**, *84*, 2167–2186. [CrossRef]

14. Grazziotin, A.; Pimentel, F.A.; De Jong, E.V.; Brandelli, A. Nutritional Improvement of Feather Protein by Treatment with Microbial Keratinase. *Anim. Feed Sci. Technol.* **2006**, *126*, 135–144. [CrossRef]

15. Staroń, P.; Banach, M.; Kowalski, Z.; Staroń, A. Hydrolysis of Keratin Materials Derived from Poultry Industry. *Proc. ECOpole* **2014**, *8*, 443–448.

16. Aranberri, I.; Montes, S.; Azcune, I.; Rekondo, A.; Grande, H.J. Fully Biodegradable Biocomposites with High Chicken Feather Content. *Polymers* **2017**, *9*, 593. [CrossRef]

17. Barone, J.R.; Schmidt, W.F.; Liebner, C.F. Compounding and Molding of Polyethylene Composites Reinforced with Keratin Feather Fiber. *Compos. Sci. Technol.* **2005**, *65*, 683–692. [CrossRef]

18. Barone, J.R. Polyethylene/Keratin Fiber Composites with Varying Polyethylene Crystallinity. *Compos. Part A* **2005**, *36*, 1518–1524. [CrossRef]

19. Infrared Spectrum of Triethyl Citrate (Sdbs No. 2909). Spectral Database for Organic Compounds. Available online: https://sdbs.db.aist.go.jp/sdbs/cgi-bin/landingpage?sdbsno=2909 (accessed on 12 March 2020).

20. Gebhard, J.; Sellin, D.; Hilterhaus, L.; Liese, A. Online-Analyse Von Enzymatischen Polykondensationsreaktionen in Blasensäulenreaktoren Mittels Atr-Ftir-Spektroskopie. *Chem. Ing. Tech.* **2013**, *85*, 1016–1022. [CrossRef]

21. Popescu, C.; Segal, E. Critical Considerations on the Methods for Evaluating Kinetic Parameters from Nonisothermal Experiments. *Int. J. Chem. Kinet.* **1998**, *30*, 313–327. [CrossRef]

22. Otton, J.; Ratton, S.; Vasnev, V.A.; Markova, G.D.; Nametov, K.M.; Bakhmutov, V.I.; Komarova, L.I.; Vinogradova, S.V.; Korshak, V.V. Investigation of the Formation of Poly (Ethylene Terephthalate) with Model Molecules: Kinetics and Mechanisms of the Catalytic Esterification and Alcoholysis Reactions. Ii. Catalysis by Metallic Derivatives (Monofunctional Reactants). *J. Polym. Sci. Part A* **1988**, *26*, 2199–2224. [CrossRef]

23. Lide, D.R. *Crc Handbook of Chemistry and Physics, 2000-2001*; CRC Press: Boca Raton, FL, USA, 2000.

24. Carothers, W.H. Polymers and Polyfunctionality. *Trans. Faraday Soc.* **1936**, *32*, 39–49. [CrossRef]

25. Noordover, B.A.; Duchateau, R.; van Benthem, R.A.; Ming, W.; Koning, C.E. Enhancing the Functionality of Biobased Polyester Coating Resins through Modification with Citric Acid. *Biomacromolecules* **2007**, *8*, 3860–3870. [CrossRef]

26. Barbooti, M.M.; Al-Sammerrai, D.A. Thermal Decomposition of Citric Acid. *Thermochim. Acta* **1986**, *98*, 119–126. [CrossRef]

27. van Krevelen, D.W. Some Basic Aspects of Flame Resistance of Polymeric Materials. *Polymer* **1975**, *16*, 615–620. [CrossRef]